Robust Digital Control for a PFC Boost Converter

Yoshihiro Ohta[1], **Kohji Higuchi**[2], and **Kosin Chamnongthai**[3], Non-members

ABSTRACT

A PFC boost converter is a non-linear system whose small perturbation model is changed at each operating point depending on a duty ratio. And when a duty ratio, a load resistance and an input voltage are changed, a small perturbation model is changed greatly. A robust controller for the PFC boost converter is needed to suppress an output voltage change at load sudden change while attaining a high power factor and a low harmonic. In this paper, the combining method and design methods of two approximate 2-degree-of-freedom (A2DOF) controllers which simplify the overall controller and attain good robustness are proposed. The proposed controller is actually implemented on a Micro-processor and is connected to the PFC boost converter. Experimental studies demonstrate that the proposed robust controller is effective to suppress the output voltage change to improve the power factor and to decrease the harmonic.

Keywords: Power Factor Correction, Boost Converter, Approximate 2DOF, Robust Control, Microprocessor

1. INTRODUCTION

Recent years, improving of a power factor and reducing a harmonic of a power supply using non-linear electrical instruments are needed. In general, electrical instruments have a rectifier that has non-linear characteristics. The rectifier occurs the descent of the power factor and the increase of harmonic distortion. The poor power factor incurs inefficient power transmission and increase equipment investment of power companies. The harmonic causes overheating of the power line, burning out of a capacitor or malfunction of a breaker. So the limit for harmonic current emissions is laid down around the world (IEC/EN61000-3-2).

A passive filter or an active filter in AC line is used for improving of the power factor and reducing the harmonic [1-2]. Usually a continuous conduction mode boost converter is used for an active PFC in electrical instruments. In a PFC boost converter, if a duty ratio, a load resistance and an input voltage are changed, the dynamic characteristics are varied greatly, that is, the PFC converter has non-linear characteristics. In many applications of the PFC converters, loads cannot be specified in advance, i.e., their amplitudes are suddenly changed from the zero to the maximum rating. These are prime reasons of difficulty for controlling the PFC boost converter.

Usually, a controller of the PFC converter is designed to an approximated linear controlled object in some neighbourhood of some operating point. Usually, in the non-linear PFC boost converter system, it is not enough to design of the controller for only one operating point. As a technique to improve dynamic performance, the gain-scheduled control is taken into consideration[3]. However, since many controllers must be designed to many operating points, it requires a complicated control routine for switching the controllers. Then, the controller which can cover sudden load changes and dynamic characteristics changes with only one controller is needed for simplifying the control system.

Simple integral controls etc. are performed in analog control. Moreover, PID or root locus method etc. [4-6] have been considered in application of digital control, but robustness is not enough. In order to improve robustness, various methods [7-9] are proposed. However, it is difficult to retain sufficient robustness and high power factor of the PFC converters in digital control by these techniques. A robust control method using an approximate 2-degree-of-freedom (A2DOF) for improving start-up characteristics and load sudden change characteristics of power converters has been proposed [10-11]. However, it was applied to a buck DC-DC converters. The PFC boost converter needs a current controller and a voltage controller. We use two A2DOF controllers for these controllers in order to suppress the output voltage change while attaining the high power factor and the low harmonic.

In this paper, the combining method and design methods of two A2DOF controllers which simplify the overall controller and attain good robustness are proposed. Firstly the current control system is constituted using the A2DOF current controller to the controlled object. Next, the current control system is approximated and the voltage control system is constituted using the A2DOF voltage controller to the

Manuscript received on April 19, 2012 ; revised on February 10, 2012.

[1,2] The authors are with Department of Mechanical Engineering and Intelligent Systems, The University of Electro-Communications 1-5-1, Chofugaoka, Chofu, Tokyo, 182-8585, Japan, E-mail: ohta@francis.ee.uec.ac.jp and higuchi@ee.uec.ac.jp

[3] The author is with King Mongkut's University of Technology Thonburi, 126 Pracha-utid Road Bangmod, Toongkru, Bangkok, Thailand, E-mail: kosin.cha@kmutt.ac.th

approximated current system. This controller is actually implemented on a Micro-processor and is connected to the PFC converter. Experimental studies demonstrate that the digital controller designed by this proposed method satisfies the given specifications and is useful practically.

2. PFC BOOST CONVERTER

2.1 State-space model of boost DC-DC converter

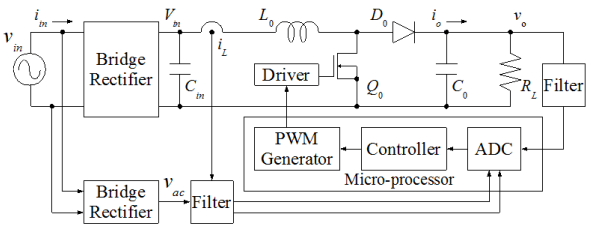

Fig.1: *Digital Controlled PFC Boost Converter.*

The PFC boost converter is shown in Fig.1. Fig.1 is including the rectifier, the smoothing circuit, continuous conduction mode DC-DC boost converter and the digital controller. In Fig.1, v_{in} is an input AC voltage, i_{in} is an input AC current, C_{in} is a smoothing capacitor, V_{in} is a rectified and smoothed input voltage, Q_0 is a MOSFET, L_0 is a boost inductance, D_0 is a boost diode, C_0 is an output capacitor, R_L is an output load resistance, i_L is an inductor current, v_{ac} is an absolute value of input AC voltage and v_o is an output voltage. Here C_{in} is 1μF, L_0 is 150μH and C_0 is 940μF. The inductor current i_L is controlled to follow the rectified input voltage v_{ac} for improving the power factor, reducing the harmonic and stabilizing the output voltage. Using a state-space averaging method, the state equation of the boost converter becomes as follows [12]:

$$\frac{d}{dt}\begin{bmatrix} i_L \\ v_o \end{bmatrix} = \begin{bmatrix} -\dfrac{R_0}{L_0} & -\dfrac{1}{L_0} \\ \dfrac{1}{C_0} & -\dfrac{1}{R_L C_0} \end{bmatrix} \begin{bmatrix} i_L \\ v_0 \end{bmatrix} + \begin{bmatrix} \dfrac{V_{in}}{L_0} \\ 0 \end{bmatrix} + \left\{ v_0 \begin{bmatrix} \dfrac{1}{L_0} \\ 0 \end{bmatrix} + i_L \begin{bmatrix} 0 \\ -\dfrac{1}{C_0} \end{bmatrix} \right\} \mu \tag{1}$$

Here, the equivalent resistance of inductor R_0 is 1.8Ω. And μ is a duty ratio. The boost converter has nonlinear characteristics because this equation has the product of the state variables v_o, i_L and the duty ratio μ.

2.2 Static characteristics of boost converter

At some operating point of eq. (1), let v_o, i_L and μ, be V_s, I_s and μs, respectively. Then the average of the output voltage Vs and the inductor current I_s at some operating point become as follows:

$$V_s = \frac{(1-\mu_s)V_{in}}{(1-\mu_s)^2 + \dfrac{R_0}{R_L}}$$
$$I_s = \frac{1}{R_L}\frac{V_s}{1-\mu_s} \tag{2}$$

The actual measurement results of the static characteristics of μ_s to V_s are shown in Fig.2. In Fig.2, it turns out that the boost converter is a non-linear system.

The static characteristics of the boost converter are changed greatly with load resistances, and its influence the dynamic characteristics of converter. In addition, the static characteristics will be changed with input voltage variation [12].

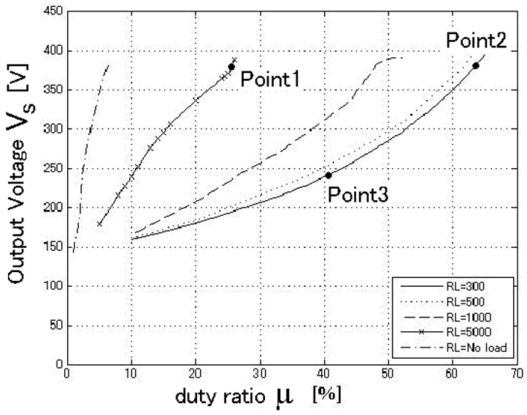

Fig.2: *Actual Static Characteristics of μ_s to V_s.*

2.3 Dynamic characteristics of boost converter

The linear approximate state equation of the boost converter using small perturbations $\Delta i_L = i_L - I_s$, $\Delta v_o = v_o - V_s$ and $\Delta\mu = \mu - \mu_s$ is as follows:

$$\begin{aligned} \dot{x}_d(t) &= A_c x_d(t) + B_c u(t) \\ y(t) &= C_c x(t) \end{aligned} \tag{3}$$

where

$$A_c = \begin{bmatrix} -\dfrac{R_0}{L_0} & -\dfrac{1-\mu_s}{L_0} \\ \dfrac{1-\mu_s}{C_0} & -\dfrac{1}{R_L C_0} \end{bmatrix}, B_c = \begin{bmatrix} \dfrac{V_s}{L_0} \\ -\dfrac{I_s}{C_0} \end{bmatrix}, C_c = \begin{bmatrix} 1 & 0 \\ 0 & 1 \end{bmatrix}$$
$$x_d(t) = \begin{bmatrix} \Delta i_L(t) \\ \Delta v_0(t) \end{bmatrix}, u(t) = \Delta\mu(t), y = \begin{bmatrix} y_i \\ y_v \end{bmatrix} = \begin{bmatrix} \Delta i_L(t) \\ \Delta v_0(t) \end{bmatrix}$$

Here, Δi_L, Δv_o, $\Delta\mu$ are small-signal variables. And $y_i, = \Delta i_L$ is a small signal inductor current and $y_v = \Delta v_o$ is a small signal output voltage.

From this equation, matrix A and B of the boost converter depends on the duty ratio μ_s. Therefore,

the converter response will be changed depending on the operating point and other parameter variations. The changes of the load R_L, the duty ratio μ_s, the output voltage V_s and the inductor current I_s in the controlled object are considered as parameter changes in eq. (3). Such parameter changes can be replaced with equivalent disturbances inputted to the input and the output of the controlled object. Therefore, what is necessary is just to constitute the control systems whose pulse transfer functions from the equivalent disturbances to the output y become as small as possible in their amplitudes in order to robustize or suppress the influence of these parameter changes.

The controller of the PFC boost converter used as power supplies for server system and inverter power supplies for Air Conditioner etc. is designed. Then the controller which satisfies the following specifications will be designed.

1. The input voltage v_i is 100VAC, And the output voltage v_o changes from 240VDC to 385VDC.
2. The step responses of the output voltage are almost the same at the resistive loads where $300 \leq R_L < 5k\Omega$, and over-shoots in these step responses are less than 10% in the step response.
3. The dynamic load response is smaller than 5% (19.3VDC) against the change of the load s between 30∼500W.
4. The power factor is over 0.99 at the full load, and the harmonics is less than the standards prescribed in IEC/EN61000-3-2.
5. The control bandwidth of a current control system is about 10kHz and the control bandwidth of a voltage control system is about 1Hz for satisfying Spec. 4.

Under these specifications, the following three operating points were selected from Fig.2 for deciding one controller.

Point 1: The output voltage is 385VDC, The resistive load is 5kΩ

Point 2: The output voltage is 385VDC, The resistive load is 300Ω

Point 3: The output voltage is 240VDC, The resistive load is 300Ω

The bode diagram of the transfer function of the controlled objects (3) at these operating points are shown in Fig.3. From this figure, the gains and phases characteristics are different at each operating point. The A2DOF controller is designed to one operating point selected from these.

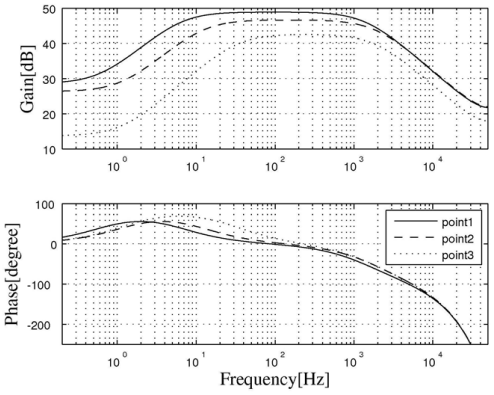

Fig.3: *Bode Diagram of $\Delta\mu$ to Δi_L.*

3. DIGITAL ROBUST CURRENT CONTROLLER

3.1 Discretization of controlled object

The continuous system of eq. (3) is transformed into the discrete system as follows:

$$\begin{aligned} x_d(k+1) &= A_d x_d(k) + B_d u(k) + q_u(k) \\ y(k) &= C_d x_d(k) + q_y(k) \end{aligned} \tag{4}$$

where

$$A_d = \left[e^{A_c T}\right], B_d = \left[\int_0^T e^{A_c \tau} B_c d\tau\right], C_d = C_c$$

Here, in order to compensate the delay time by an A/D conversion time and a micro-processor operation time etc., one delay (state ξ_1) is introduced to input of the controlled object. Then, a new controlled object with one delay is shown in Fig.4. In Fig.4, q_v and q_y are the equivalent disturbances with which the parameter changes of the controlled object are replaced.

The state-space equation is described as follows:

$$\begin{aligned} x_{dt}(k+1) &= A_{dt} x_{dt}(k) + B_{dt} v(k) \\ y(k) &= C_{dt} x_{dt}(k) \end{aligned} \tag{5}$$

where

$$\begin{aligned} A_{dt} &= \begin{bmatrix} e^{A_c T_s} & e^{A_c(T_s - L_d)} \int_0^{L_d} e^{A_c \tau} B_c d\tau \\ 0 & 0 \end{bmatrix} \\ &= \begin{bmatrix} a_{11} & a_{12} & a_{13} \\ a_{21} & a_{22} & a_{23} \\ 0 & 0 & 0 \end{bmatrix} \\ B_{dt} &= \begin{bmatrix} \int_0^{T_s - L_d} e^{A_c \tau} B_c d\tau \\ 1 \end{bmatrix} = \begin{bmatrix} b_{11} \\ b_{21} \\ 1 \end{bmatrix} \\ C_{dt} &= \begin{bmatrix} C_d & 0 \end{bmatrix} \\ x_{dt}(k) &= \begin{bmatrix} x_d(k) \\ \xi_1(k) \end{bmatrix} = \begin{bmatrix} \Delta i_L(k) \\ \Delta v_o k \\ u(k) \end{bmatrix} \end{aligned}$$

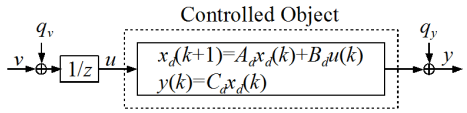

Fig.4: *Discrete-time Controlled Object with Input Delay.*

3.2 Design method for A2DOF digital current controller

The transfer function from the reference input r_i' to the output y_i is specified as follows:

$$W_{r_i' y_i}(z) = \frac{(1-H_1)}{z+H_1}\frac{(1-H_2)}{z+H_2}\frac{(1-H_3)}{z+H_3} \times \frac{(z-n_{1i})}{1+n_{1i}}\frac{(z-n_{2i})}{1+n_{2i}} \tag{6}$$

Here $H_i, i = 1, 2, 3$ are the specified arbitrary parameters, n_{1i} and n_{2i} are the zeros of the discrete-time controlled object. This target characteristic $W_{r_i' y_i}$ is realizable by constituting the model matching system shown in Fig.5 using the following state feedback to the controlled object (5).

$$v = -Fx_{dt} - G_i r_i \tag{7}$$

Here $F = [f_1\ f_2\ f_3]$ and G_i are selected suitably.

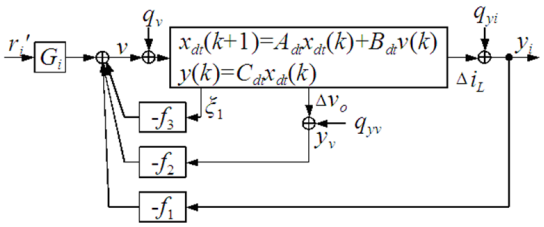

Fig.5: *Model matching system using state feedback.*

It shall be specified that the relation of H_1 and H_3 become $|H_1| \gg |H_3|$ and $n_{1i} \approx H_2$. Then $W_{r_i' y_i}$ can be approximated to the following first-order discrete-time model:

$$W_{r_i' y_i}(Z) \approx W_{mi}(z) = \frac{1+H_1}{z+H_1} \tag{8}$$

The system added the inverse system and the filter to the system in Fig.5 is constituted as shown in Fig.6.

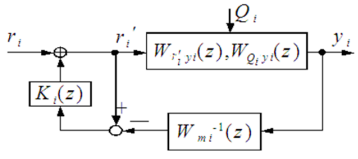

Fig.6: *System Reconstituted with Inverse System and Filter.*

In Fig.6, the transfer function $K_i(z)$ is as follows:

$$K_i(z) = \frac{k_{z_i}}{z-1+k_{zi}} \tag{9}$$

The transfer function $W_{Qyi}(z)$ between the equivalent disturbance $Qi = [q_v\ q_{yi}^T]$ to y_i of the system in Fig.6 is defined as

$$W_{Qiyi}(z) = \lfloor W_{qvyi}(z) \quad W_{qyiyi}(z) \rfloor \tag{10}$$

The transfer functions between $r_i - y_i, q_v - y_i$ and $q_{yi} - y_i$ of the system in Fig.6 are given by

$$y_i = \frac{1+H_1}{z+H_1}\frac{z-1+k_{zi}}{z-1+k_{zi}W_{si}(z)}W_{si}(z)r_i \tag{11}$$

$$y_i = \frac{z-1}{z-1+k_{zi}}\frac{z-1+k_{zi}}{z-1+k_{zi}W_{si}(z)}W_{Qyi}(z)Q_i \tag{12}$$

where

$$W_{si}(z) = \frac{(1+H_3)}{(z+H_3)}\frac{(z-n_{1i})}{(1-n_{1i})}$$

Here, if $W_{si}(z) \approx 1$, then eq. (11) and eq. (12) are approximated, respectively as follows:

$$y_1 \approx \frac{1+H_1}{z+H_1}r_i \tag{13}$$

$$y_i = \frac{z-1}{z-1+k_{zi}}W_{Qiyi}(z)Q_i \tag{14}$$

From eq. (13), (14), it turns out that the characteristics from r_i to y_i can be specified with H1 and the characteristics from Q_i to y_i can be independently specified with k_{zi}. That is, the system in Fig.6 is the A2DOF system, and its sensitivity against disturbances becomes lower with the increase of k_{zi}. If the equivalent conversion of the controller in Fig.6, we obtain Fig.7.

Then, substituting a system of Fig.5 to Fig.7, the A2DOF digital integral type control system will be obtained as shown in Fig.8. In Fig.8, the parameters of the controller are as follows:

$$\begin{aligned} &k_1 = -f_1 - \frac{G_i k_{zi}}{1+H_1},\ k_2 = -f_2 \\ &k_3 = -f_3,\ k_{ii} = G_i k_{zi},\ k_{ri} = G_i \end{aligned} \tag{15}$$

3.3 Design of current controller parameters

The sampling period was set to $T_s = 10\mu s$ and the delay time is $L_d = 0.99\ T_s$. The controller is designed to eq. (5) of the operating point 2 as the nominal model. First of all, determine the parameter H_1, H_2 and H_3 to satisfy Spec.5 as follows:

$$H_1 = -0.5, H_2 = -0.999927 \approx n_{2i}, H_3 = 0.2 \tag{16}$$

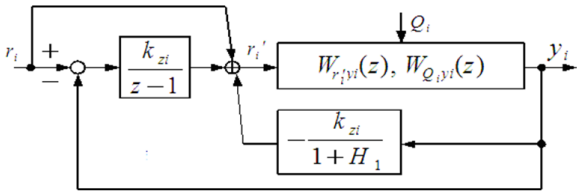

Fig.7: *Equivalent Conversion of the Robust Digital Controller.*

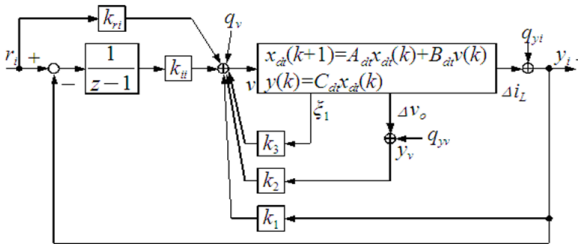

Fig.8: *Approximate 2DOF Digital Integral Type Current Control System.*

Next, determine k_{zi} using the root locus. The poles of the system of Fig.8 change with the increases in kzi. The root loci are shown in Fig.9. In Fig.9, p1i, p2i are the poles of this system of Fig.8 in case kzi is set to some value. H_1, H_2 are the poles which are not moved since it is eliminated in root locus. The poles p1i, p2i should be inside of unit circle in z-plane and satisfy the condition of $|H_1| \gg (|p_{1i}|, |p_{2i}|)$ and producing only slight over shoot in step response. So k_{zi} is set to 0.35. Then the parameters of controller become as follows:

$$\begin{aligned} &k_1 = -0.034705, \quad k_2 = 0.0014317, \\ &k_3 = -0.828241, \quad k_{ii} = 0.0086668, \\ &k_{ri} = 0.024762 \end{aligned} \tag{17}$$

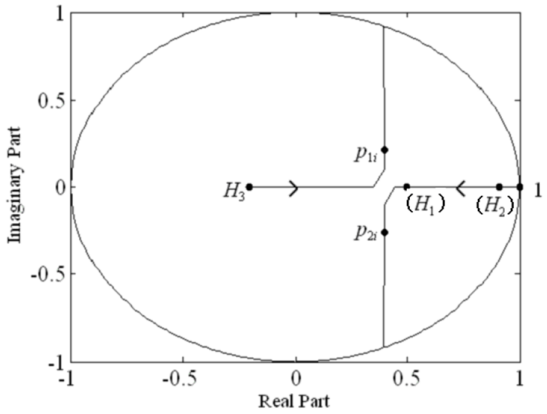

Fig.9: *Root Locus of the Current Control System at nominal system(operating point 2).*

4. DIGITAL ROBUST VOLTAGE CONTROLLER

4.1 Addition of u_v and v_{ac} to r_i

Add the multiplier in front of the reference input r_i of the current control system. Let the inputs of the multiplier be v_{ac} and u_v as shown in Fig.10. v_{ac} is the absolute value of the input voltage v_{in} and u_v is a new input. This addition is for making the inductor current i_L follow the AC voltage v_{ac}.

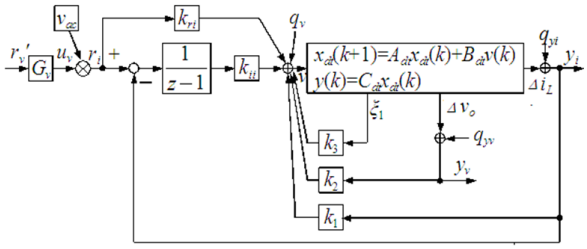

Fig.10: *Current Control System Added Multiplier.*

4.2 Approximate controlled object for voltage controller

The system of Fig.10 becomes a controlled object for a voltage controller. Derive an approximated controlled object from this system for designing the voltage controller. In Fig.10, u_v is a control input, and $\Delta v_o = y_v$ is an output of the controlled object. When u_v is set to $u_v = G_v r'_v$, the transfer function from r_v' to v_o is as follows:

$$\begin{aligned} v_o = &\frac{(1+H_2)}{(z+H_2)}\frac{(1+H_1)}{(z+H_1)}\frac{(1+p_{1i})}{(z+p_{1i})}\frac{(1+p_{2i})}{z+p_{2i}} \\ &\times\frac{(z-n_{1v})}{(1-n_{1v})}\frac{(z-n_{2v})}{(1-n_{2v})}r'_v = W_{ryv}r'_v \end{aligned} \tag{18}$$

where

$$G_v = \frac{1}{G_{uv}} = \frac{a_{21} + \dfrac{a_{23}}{G_{ui}} + \dfrac{b_{21}}{G_{ui}}}{1-a_{22}}, G_{ui} = \frac{1}{C_{dt}(I-A_{dt})^{-1}B_{dt}}$$

G_{uv} is DC gain between u_v to v_o. n_{1v}, n_{2v} are zeros of the transfer function from u_v to v_o.

In eq. (18), $|H_2| \gg (|H_1|, |p_{1i}|, |p_{2i}|)$, so the controlled object $W_{rv'yv}$ for the voltage controller is approximated as:

$$W_{rv'yv}(z) \approx W_{mv}(z) = \frac{1+H_2}{z+H_2} \tag{19}$$

4.3 Design method of A2DOF voltage controller

The inverse system $W_{mv}^{-1}(z)$ and the filter $K_v(z)$ are added to the system of eq. (18) like Fig.6. Here $K_v(z)$ is as follows:

$$K_v(z) = \frac{k_{zv}}{z - 1 + k_{zv}} \tag{20}$$

In Fig.6, r_i, y_i, Q_i, q_v, q_{yi}, K_i, W_{ryi}, W_{mi}^{-1}, and W_{Qiyi} are replaced with r_v, y_v, Q_v, q_v, q_{yv}, K_v, W_{ryv}, W_{mv}^{-1}, and W_{Qvyv}, respectively. Then the transfer functions between $r_v - y_v$, $q_v - y_v$ and $q_{yv} - y_v$ of the system in Fig.6 are given by

$$y_v \approx \frac{1 + H_2}{z + H_2} r_v \tag{21}$$

$$y_v \approx \frac{z - 1}{z - 1 + k_{zv}} W_{Qvyv}(z) Q_v \tag{22}$$

The A2DOF digital integral type control system will be obtained from the equivalent conversion of the controller like Fig.6 as shown in Fig.11. All specifications will be satisfied with only one controller of Fig.11.

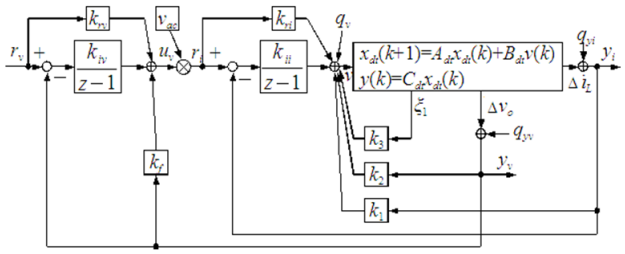

Fig.11: *Approximate 2DOF Digital Integral Type Control System Including the Current Controller and the Voltage Controller.*

In Fig.11, the parameters of the voltage controller are as follows:

$$k_f = -\frac{G_v k_{zv}}{1 + H_2}, k_{iv} = G_v k_{zv}, k_{rv} = G_v \tag{23}$$

4.4 Design of voltage controller parameters

H_2 is set as eq. (16). Next, determine k_{zv} using the root loci and the closed loop transfer function from r_i to i_L . In the system of Fig.11, the poles almost do not move on the loci even if k_{zv} increases. The pole moved from -1 is cancelled by the zeros of W_{mv}^{-1}. That is, regardless of k_{zv}, the transfer functions between $r_v - y_v$ of the system in Fig.11 become almost equal to eq. (18). The bode diagram of the transfer function from r_i to Δi_L in the PFC control system of Fig.11 are shown in Fig.12 when k_{zv} is set to 0.25. In Fig.12, the cut-off frequencies f_{cl} is $f_{cl} \ll$ 50Hz. So the current control system is hardly influenced by the voltage controller. Then the controller parameters become as follows:

$$\begin{aligned} &k_f = -45.153, k_{iv} = 0.0032900 \\ &k_{rv} = 0.01316 \end{aligned} \tag{24}$$

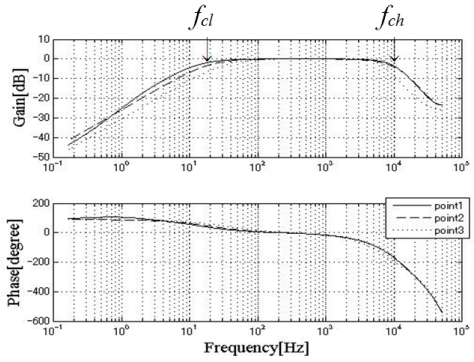

Fig.12: *Bode diagram from r_i to Δi_L of the System in Fig.11.*

5. SIMULATION AND EXPERIMENTAL RESULTS

The simulation results of 20V step response are shown in Fig.13. It turns out that even if the controlled objects are changed for the change of the operating points, the responses are not changed and they have no over-shoot. The rising time of the output voltage are about 400ms. The simulation results of the steady state waveform of the inductor current are shown in Fig.14. The inductor current waveform is almost same as the rectified input voltage. The simulation results of the output voltage and the output current at the sudden load changes from 1kΩ to 300Ω(150W to 500W) are shown in Fig. 15. The output voltage variation is less than 10V.

Experimental setup system is shown in Fig.16. A Micro-processor (SH7216) from Renesas Electronics Corp. is used for the controller.

The experimental results of 20V step responses at each operating points are shown in Fig.17. It turns out that even if the operating point changes, the step responses are not change and it satisfy Spec.2.

The experiment result of the steady state at operating point 2 is shown in Fig.18. The input current waveform and the phase are the almost same as the input voltage and the power factor of converter at the full load is 0.994. The power factor at various loads is shown in Fig.19. The harmonic characteristic at full load is shown in Fig.20 and it is less than the standards in the all the frequencies. This result shows that the controller satisfies Spec.4.

The experiment result of load sudden change using the proposed controller is shown in Fig.21. In Fig.21, the output voltage variation in sudden load change is less than 10V (2.60%), and it satisfies Spec.3. The experiment result of load sudden change between 1kΩ to 300Ω using the PI controller is shown in Fig.22. The output voltage variation is over 20VDC (5.19%). From these results, the control system using PI controller cannot satisfy specification. As a result, it turns out that the proposed controller is effective practically.

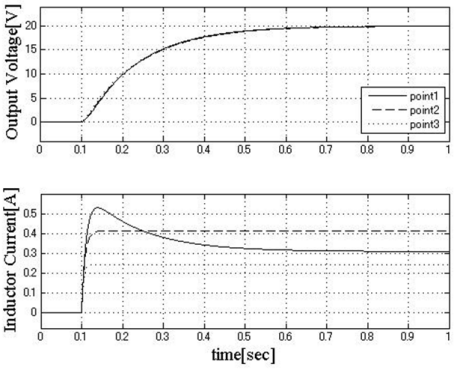

Fig.13: *Simulation Results of Step Responses.*

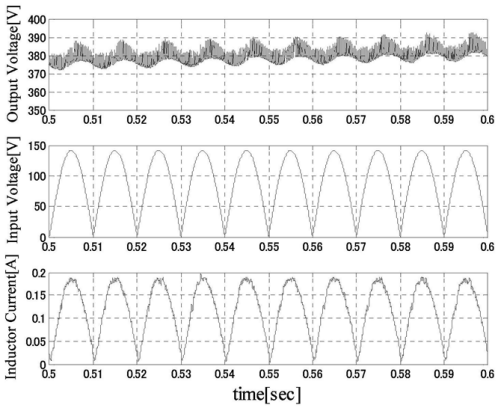

Fig.14: *Simulation Results of Steady State Waveform.*

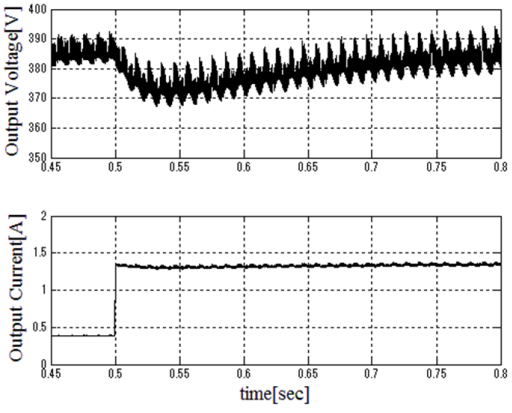

Fig.15: *Simulation Results of Steady State Waveform.*

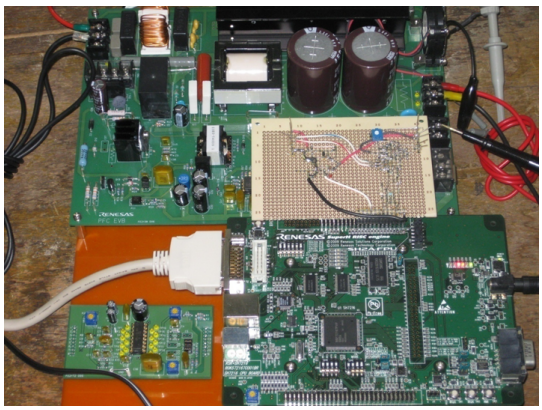

Fig.16: *Experimental setup system.*

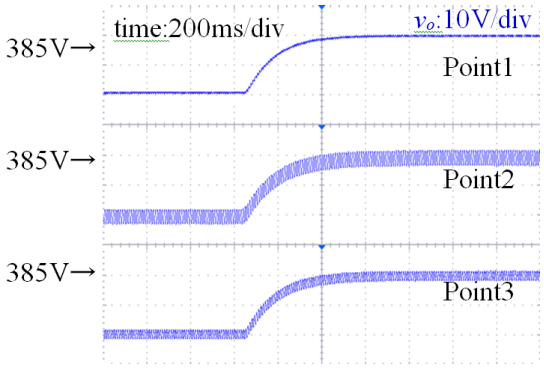

Fig.17: *Experimental Results of Step Responses at Each Operating Point.*

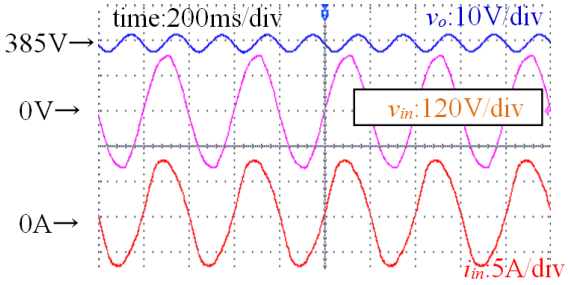

Fig.18: *Experimental Results of Steady State Waveform.*

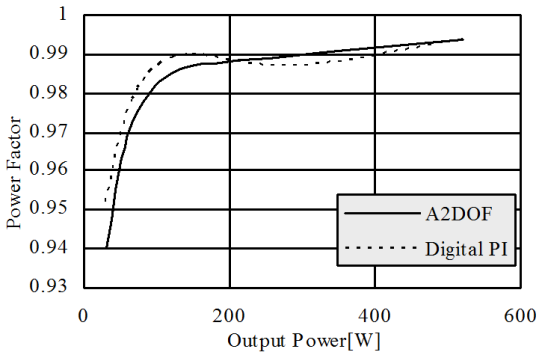

Fig.19: *Power Factor Characteristics.*

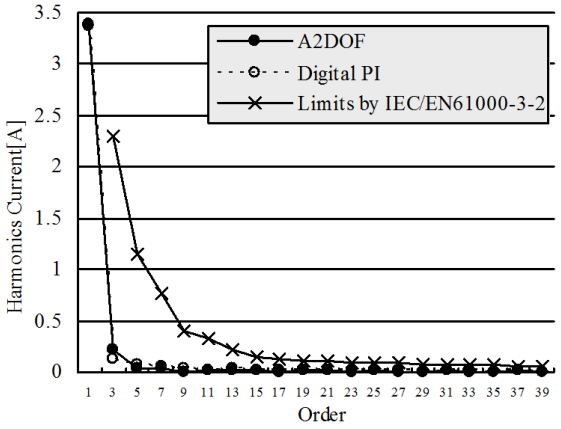

Fig.20: *Harmonics Performance at Full Load (500W).*

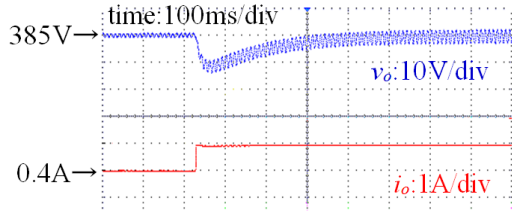

Fig.21: *Experimental Results of Sudden Load Change From 1kΩ to 300Ω , where Using A2DOF Controller.*

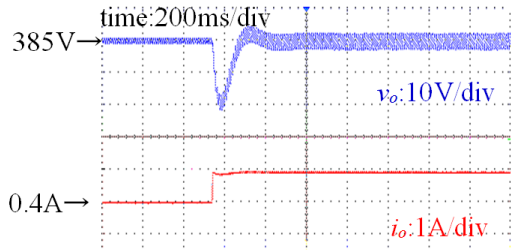

Fig.22: *Experimental Results of Sudden Load Change From 1kΩ to 300Ω, where Using PI Controller.*

6. CONCLUSION

In this paper, the concept of the digital controller which attains good robustness for the non-linear PFC boost converter was given. The proposed digital controller was implemented on the micro-processor. The PFC boost converter built-in this micro-processor was manufactured. It was shown from simulations and experiments that the digital controller which combined two A2DOF can suppress the variations of the step responses at load change and the output voltage variations at sudden load changes while attaining the high power factor and the low harmonic. This fact demonstrates the usefulness and practicality of our proposed method. A future subject is checking experimentally the change of the output voltage when the input voltage is changed.

References

[1] L. Rossetto, G. Spiazzi, and P. Tenti, "Control Techniques for Power Factor Correction Converters", *Proc. PEMC'94*, pp.1310–1318, 1994.

[2] M. Xie, "Digital Control For Power Factor Correction," *Unpublished master's thesis*, Virginia Polytechnic Institute and State University, 2003.

[3] E. D. Bolat, K. Erkan, S. Postalcioglu, "Using Current Mode Fuzzy Gain Scheduling Of PI Controller for UPS Inverter," *IEEE EUROCON 2005*, pp.1505–1508, 2005.

[4] M. Fu and Q. Chen, "A DSP Based Controller for Power Factor Correction (PFC) in a Rectifier Circuit," *IEEE APEC 2001*, pp.144–149, 2001.

[5] K. De Gusseme, D. M. Van de Sype and J. A. A. Melkebeek "Design Issues for Digital Control of Boost Power Factor Correction Converters," *IEEE ISIE 2002*, pp.731–736, 2002.

[6] W. Zhang, G. Feng, Y. Liu and B. Wu, "A Digital Power Factor Correction (PFC) Control Strategy Optimized for DSP," *IEEE Transactions on Power Electronics*, vol. 19, no. 6, pp.1474–1485, 2004.

[7] E. Figueres, J. M. Benavent, G. Garcera and M. Pascual, "A Control Circuit With Load-Current Injection for Single-Phase Power-Factor-Correction Rectifiers," *IEEE Transactions on Industrial Electronics*, vol. 54, no. 3, pp.1272–1281, 2007.

[8] A. de Castro, P. Zumel, O. Garcia, T. Riesgo and J. Uceda "Concurrent and Simple Digital Controller of an AC/DC Converter With Power Factor Correction Based on an FPGA," *IEEE Transactions on Power Electronics*, vol. 18, no. 1, pp.334-343, 2003.

[9] S. Buso, P. Mattavelli, L. Rossetto and G. Spiazzi "Simple Digital Control Improving Dynamic Performance of Power Factor Preregulators," *IEEE Transactions on Power Electronics* , vol. 13, no. 5, pp.814–823, 1998.

[10] K. Higuchi, K. Nakano, T. Kajikawa, E. Takegami, S. Tomioka, K. Watanabe, "A New Design of Robust Digital Controller for DC-DC Converters," *IFAC 16th Triennial World Congress*, (CD-ROM), 2005.

[11] K. Higuchi, E. Takegami, K. Nakano, T. Kajikawa, S. Tomioka, "Digital Robust Control for DC-DC Converter with Second-Order Characteristics," *ECTI-CON'2009*, pp.161–169, 2009.

[12] S. Sasaki, and H. Watanabe, "Analysis of Multiple Operating Points for Dynamical Control of Switching Power Converters," *IEIC Technical Report*, pp.33–38, 2005.

Yoshihiro Ohta received his B.S. degree from The University of Electro-Communications, Tokyo, Japan, in 2010. In 2012, he is M.S. degree student of the Dept. of Mechanical Engineering and Intelligent Systems, the University of Electro-Communications. His research interests include Power Electronics, Control Engineering, Digital Signal Processing and Embedded Systems Design. He is a student member of SICE and IEICE.

Kohji Higuchi received his Ph.D. degree from Hokkaido University, Sapporo, Japan in 1981. In 1980 he joined the University of Electro-Communications, Tokyo, Japan, as an Research Associate, where he became an Assistant Professor in 1982 and currently an Associate Professor in the Dept. of Mechanical Engineering and Intelligent Systems, Electronic Control System Course. His interests include Power Electronics, Control Engineering and Digital Signal Processing. He is a member of IEEE, IEICE, SICE and IEEJ.

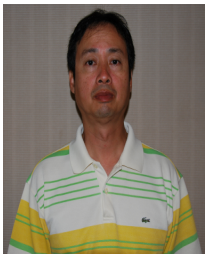

Mongkol Konghirun currently works as associate professor at Electronic and Telecommunication Engineering Department, Faculty of Engineering, King Mongkut's University of Technology (KMUTT), and also serves as editor of ECTI e-magazine, and associate editor of ELEX (IEICE Trans) during 2008-2010 and ECTI-CIT Trans since 2011 until now. He served as assoc editor of ECTI-EEC Trans during 2003-2010, and chairman of IEEE COMSOC Thailand during 2004-2007.

In organizing conference, he has served as general chair of international and national conferences such as SISA 2012, ITC-CSCC 2010, NICOGRAPH 2008, ISPACS 2008, ICESIT 2008, ICESIT 2007, IWAIT 2007, and 30th EECON.

He has recieved B.Eng. in Applied Electronics from the University of Electro-communications, Tokyo, Japan in 1985, M.Eng. in Electrical Engineering from Nippon Institute of Technology, Saitama, Japan in 1987 and D.Eng. in Electrical Engineering from Keio University, Tokyo, Japan in 1991. His research interests include image processing, computer vision, robot vision, and signal processing. He is a senior member of IEEE, and a member of IPS, TRS, IEICE, TESA and ECTI.